Appl Microbiol Biotechnol (2015) 99:4785–4794
DOI 10.1007/s00253-015-6445-0

The feasibility of using irreversible electroporation to introduce pores in bacterial cellulose scaffolds for tissue engineering

Adwoa Baah-Dwomoh · Andrea Rolong · Paul Gatenholm · Rafael V. Davalos

Received: 19 November 2014 / Revised: 27 January 2015 / Accepted: 28 January 2015 / Published online: 18 February 2015

Abstract This work investigates the feasibility of the use of irreversible electroporation (IRE) in the biofabrication of 3D cellulose nanofibril networks via the bacterial strain *Gluconacetobacter xylinus*. IRE uses electrical pulses to increase membrane permeability by altering the transmembrane potential; past a threshold, damage to the cell becomes too great and leads to cell death. We hypothesized that using IRE to kill the bacteria at specific locations and particular times, we could introduce conduits in the overall scaffold by preventing cellulose biosynthesis locally. Through mathematical modeling and experimental techniques, electrical effects were investigated and the parameters for IRE of *G. xylinus* were determined. We found that for a specific set of parameters, an applied electric field of 8 to 12.5 kV/cm, producing a local field of 3 kV/cm, was sufficient to kill most of the bacteria and create a localized pore. However, an applied electric field of 17.5 kV/cm was required to kill all. Results suggest that IRE may be an effective tool to create scaffolds with appropriate porosity for orthopedic applications. Ideally, these engineered scaffolds could be used to successfully treat osteochondral defects.

Keywords Bacterial cellulose · Irreversible electroporation · Scaffolds for tissue engineering · Biofabrication

Introduction

Tissue engineering, specifically through the use of biomaterials, provides a promising alternative to tissue harvesting by incorporating cells with bio-engineered scaffolds that mimic the extracellular matrix (Mooney and Mikos 1999; Place et al. 2009; Yang et al. 2001). Multiple techniques such as sintering, salt leeching, gas foaming, and electrospinning have been used to create micro structured architectures within scaffolds (Ellis and Yannas 1996; Gauvin et al. 2012; Harris et al. 1998; Matthews et al. 2002). However, the ability to create functional 3D tissue structures remains a challenge in the field due to the limitation of incorporating mass transport properties, such as nutrient and gas exchange. Engineered tissue constructs currently limit gas exchange to distances of less than 1 mm which is only adequate to maintain viability of simpler structures such as flat tissue layers and hollow organs. The aforementioned techniques allow for fairly uniform pore distribution but they do not allow for proper pore interconnectivity, which fails to induce microvasculature formation (Karageorgiou and Kaplan 2005; Murphy et al. 2010). This limitation needs to be overcome by creating an appropriate porosity and microvasculature throughout the bio-engineered scaffold that can support complex tissues and organs such as the liver, kidneys, and bone.

We propose the use of bacterial cellulose (BC), a nanobiomaterial produced by *Gluconacetobacter xylinus*, as the

Adwoa Baah-Dwomoh and Andrea Rolong contributed equally to this work.

A. Baah-Dwomoh · R. V. Davalos
Materials Science and Engineering, Virginia Tech, Blacksburg, VA, USA

A. Baah-Dwomoh
e-mail: adj2288@vt.edu

A. Rolong · P. Gatenholm · R. V. Davalos (✉)
School of Biomedical Engineering and Sciences, Virginia Tech—Wake Forest University, 329 Kelly Hall, 325 Stanger Street (MC 0298), Blacksburg, VA 24061, USA
e-mail: davalos@vt.edu

P. Gatenholm
BC Genesis LLC, Blacksburg, VA, USA

scaffold construct to treat cartilage and bone defects. Bone defects can arise due to age, trauma, disease, or congenital defects. Typically, when a bone defect or trauma occurs, both bone and cartilage are damaged. Cartilage does not have the same regenerative capabilities as bone, which makes the use of autologous tissue—tissue transplanted from one site in the patient to another—a less viable treatment option. Untreated cartilage lesions lead to joint defects and the development of osteoarthritis, a degenerative joint disease affecting over 9 million people in the USA alone (Katz and Losina 2013). To create a tissue-engineered cartilage replacement, a suitable biomaterial needs to be developed to help with adherence and migration of chondrocytes. BC has gained interest in the biomaterials field due to its proven biocompatibility and stability under a wide range of conditions (Helenius et al. 2006). BC has received FDA approval for surgical meshes and is currently being marketed as an antimicrobial wound dressing (Petersen and Gatenholm 2011). It is already successfully used for clinical applications such as dura replacement (Mello et al. 1997). Several studies have shown the use of BC for tissue-engineered bone grafts, cartilage, and blood vessels (Azuma et al. 2007; Czaja et al. 2007; Petersen and Gatenholm 2011; Schumann et al. 2009). Because of its good mechanical properties, such as high compressive strength, BC can withstand compressive forces similar to those experienced on the bone while closely matching the mechanical properties of the native tissue, which will allow for proper integration (Yamanaka et al. 1989).

One of the challenges of using BC as a scaffold for tissue engineering has been the densely packed network of cellulose nanofibrils that are produced by the bacteria. This study proposes the use of irreversible electroporation (IRE) as a novel biofabrication method to incorporate porosity into the BC scaffold. A previous study conducted by Sano et al. used electrokinetic forces to control bacterial motion of *Gluconacetobacter xylinus* which allowed for different orientations and organization of the cellulose fibers. This can in turn modulate the mechanical properties of the resulting construct and provide a means to fabricate customizable networks (Sano et al. 2010). Here, we focus on introducing porosity in the BC scaffold by inducing much higher electric fields to kill the bacterium rather than control its motion. We hypothesize that using IRE to kill the bacteria in specific locations and at particular times during cellulose production, we can introduce conduits in the overall scaffold by preventing cellulose deposition at these sites. IRE uses electromagnetic fields to increase the cell's transmembrane potential (TMP), thus disrupting the membrane and causing damages beyond the point of recovery, leading to cell death. Several studies have shown that IRE was used within in vitro cellular systems, in particular for sterilization in the food industry and the preprocessing of food (Sobrino-Lopez and Martin-Belloso 2006; Toepfl et al. 2006). A study conducted by Gusbeth et al. showed the effectiveness of pulsed electric field treatment for decontamination of hospital wastewater, which is full of pathogenic and antibiotic resistant bacteria (Gusbeth et al. 2009). IRE is also currently used as a tissue ablation technique in cancer treatment. Its non-thermal mechanism of inducing cell death renders the technology safe to kill tumors close to nerves and vessels (Garcia et al. 2011; Neal et al. 2010). A typical IRE procedure involves the use of a pair of electrodes inserted into the tissue to deliver microsecond-long pulses, at a specific voltage and frequency, to control the distribution of the electric field (i.e., delineation of lesion area) in the target tissue (Davalos et al. 2005). The electric field distribution is dependent on several parameters including conductivity and permeability of the tissue, number and frequency of pulses delivered, applied voltage, duration of treatments, electrode geometry, and distance between the electrodes. To achieve a specific pore geometry within the 3D BC scaffold, it is necessary to insert electrodes at the region of interest and deliver a series of pulsed electric fields to kill the bacteria.

Here, we present an innovative method for generating a 3D tissue construct with the ability to mimic native tissue microarchitecture. The use of IRE allows for a high degree of control in the topology of the design, which is typically not found in traditional biofabrication methods. By varying certain parameters such as the voltage applied, number of pulses, frequency, and duration between treatments, we can create a localized pore in the scaffold. In vitro experiments were conducted to predict cell death threshold. A finite element model (FEA) of BC pellicles was created to predict lesion volumes on the cellulose scaffolds treated with different IRE parameters. Based on these models, a series of localized electrical pulses with varying voltage and treatment time were administered to create a variable sized conduit. The results suggest that IRE may be an effective way to create bio-engineered scaffolds with appropriate porosity for orthopedic applications. Ideally, these engineered BC scaffolds could be used to successfully treat osteochondral defects in a single minimally invasive surgery.

Mathematical theory

Determination of TMP threshold

As described by Kotnik and Miklavcic (Kotnik and Miklavcic 2000), and Gisma and Wachner (Gimsa and Wachner 2001), the induced TMP on spheroidal cells can be determined by considering the presence of a homogeneous electric field E_0

being disrupted by the presence of a cell into an electric field E:

$$E = -\nabla\varphi \quad (1)$$

where φ is the electric potential and satisfies the Laplace equation

$$\nabla^2\varphi = 0 \quad (2)$$

The TMP, $\Delta\varphi$, induced by the external electric field on a bacterium is taken as the difference between the electric potential at the inner and outer surfaces of the membrane

$$\Delta\varphi = \varphi_i - \varphi_e \quad (3)$$

where the subscripts i and e denote the cell interior and exterior, respectively. Based on previous studies, a TMP>1 V must be achieved for IRE to occur (Davalos et al. 2005; Kotnik and Miklavcic 2000).

Analytical solution of electric field distribution

The local electric field produced by the pair of electrodes needs to be above a certain threshold for IRE to occur. Analytically, the electric field distribution caused by the electrical pulses can be determined. An analytical solution using the Laplace equation for a simplified 2D, two-needle electrode setup was presented in detail by Corovic et al. (Corovic et al. 2007). The Laplace equation can be solved in two-dimensions if the electrodes are assumed to be of uniform thickness, with a circle radius, a, and with a distance, d, between the electrodes that are less than the needle penetration depth. The BC is assumed to have constant conductivity, making the solution of the Laplace equation for potential of the needles:

$$\nabla^2\varphi(x,y) = 0 \quad (4)$$

where φ(x,y) is the electric potential. φ(x,y) can be rewritten as the sum of potentials generated by each needle based on superposition.

$$\varphi(x,y) = \sum_{n=1}^{N} \varphi_n(x,y) \quad (5)$$

Then, assuming two electrodes (n=2), the electric field can be determined by taking the derivative of φ(x,y). The final local electric field is determined to be:

$$E(x,y) = \frac{V_0}{2*\ln\left(\frac{d}{a}\right)} * \left[\frac{1}{a} - \frac{1}{d}\right] \quad (6)$$

where V_0 is the applied electrical potential.

Materials and methods

Bacteria cell culture

The bacteria strain *G. xylinus* (700178, American Type Culture Collection) was used for all experiments. The culture media contained modified fructose media with an addition of corn steep liquid, with a pH of 5.5 (Bodin et al. 2007; Sano et al. 2010). Cellulose forming cultures were placed in 50 mL conical tubes and incubated at 30 °C for 4 days. After 4 days, the pellicles were pushed into culture media and stirred with a cell lifter to liberate bacteria cells. Bacteria cells were then taken from suspension to conduct in vitro studies or placed in a 12-well plate to conduct the IRE pulse delivery studies on the forming cellulose pellicles.

Determination of cell death threshold by induced electric field

Bacterial cells were taken from cell suspension and centrifuged at 10,000×*g*. Cells were then resuspended in a sucrose buffer to a concentration of approximately 3×10^6 cells/mL. Ninety microliters cell suspension samples were loaded into cuvettes with 1 mm gap parallel plate electrodes, and electrical pulses were delivered using a BTX® Square Wave Electroporation System with a safety stand (Harvard Apparatus, Holliston, MA). The pulse duration (100 μs), number of pulses (1000), and interval between pulses (1 s) were held constant. The applied voltages used were 1250, 1500, and 1750 V to achieve an applied electric field of 12.5, 15, and 17.5 kV/cm. Untreated cells and cells soaked in CAVICIDE™ (Metrex, Orange, CA), a medical grade surface disinfectant/decontaminant cleaner, were used as negative and positive controls, respectively. After IRE pulse delivery, 5 μL of the bacteria suspension was placed on agar and incubated at 30 °C, yielding an approximate seeding density of 1.5×10^4 cells/agar plate. The positive and negative controls were also seeded at 1.5×10^4 cells/agar plate. Agar plates were prepared using the bacteria culture media mixed with Agar (Fisher Scientific, Pittsburgh, PA) to a concentration of 4 % agar. Agar plates were inspected at 48 and 72 h to check for bacteria cell growth and coverage. Cells were imaged macroscopically using an Olympus EVOLT E-410 Digital Single-

lens Reflex camera (Olympus Co., Center Valley, PA). A MATLAB (MathWorks, Natick, MA) script was written to determine the percent coverage of the bacteria on the agar, i.e., a direct correlation to percent growth. Statistical differences between treatments were evaluated using one-way analysis of variance (ANOVA) and Tukey's HSD test for multiple comparisons ($n=3$, $p<0.05$).

IRE pulse delivery on BC scaffold

Four pairs of stainless steel electrodes, 300 μm in diameter with 1 mm spacing, were placed in the active cultures of *G. xylinus* in four wells of a 12-well polystyrene plate (radius 1.5 cm) and then incubated at 30 °C for 48 h to allow pellicle growth of approximately 2 mm. Three wells were treated concurrently and the fourth well was taken as a control. Electrical pulses were delivered through the BTX® system every 15 to 60 min at varying voltages of 800, 1000, and 1250 V and treatment periods of 12–72 h. Parameters, such as the number of pulses (90), interval between pulses (1 s), and duration of pulse (10 μs) were kept constant. After completion of treatment, pellicles were harvested, washed with 0.1 M NaOH at room temperature for 24 h, and rinsed with DI water.

Pellicles were imaged macroscopically and lesion area was determined using ImageJ (NIH, Bethesda, MD). In addition to macroscopic imaging, pellicles were imaged with field emission scanning electron microscopy (FESEM). Pellicles were frozen at −80 °C for 24 h, freeze dried in a Labconco FreeZone 3 (Labconco Corp., Kansas City, Missouri) for 48 h, and coated with 5 nm gold palladium for FESEM. FESEM was conducted at a working distance of 12 mm and 5 kV electron beam intensity using a LEO Zeiss 1550 FESEM (Carl Zeiss SMT, Oberkochen, Germany).

Numerical model of lesion area

A FEA model (COMSOL Multiphysics 4.3a, Boston, MA) was used to calculate and estimate the electric field distribution experienced on the BC. A 2D model represented electrode placement in the cellulose pellicle where one electrode was set to have a constant voltage at steady state and the other electrode set to ground. The dimensions of the stainless steel electrodes (300 μm diamater) and the pellicle (1.5 cm diameter) were selected to match the experimental conditions described in the previous section, with the whole pellicle being the region of interest. The pellicle was set to act as an insulating boundary. The applied voltages were selected to simulate an applied electric field of 10 and 12.5 kV/cm for an electrode spacing of 1 mm. The electrical conductivity of the pellicle was set to 2 S/m (Yoon et al. 2006). An extra fine mesh was used that consisted of 8934 triangular elements.

Results

Determination of cell death threshold by induced electric field

The bacteria were reseeded on agar plates after electroporation to determine cell viability (Fig. 1). Cells were electroporated at 12.5, 15, and 17.5 kV/cm to determine the cell death threshold. The agar plates were inspected at 48 and 72 h after electroporation to determine the effect of electroporation on cell growth. The mean percent coverage of the untreated bacteria, which served as the negative control, was 29.48±6.162 (mean ±SD) % after 48 h and 45.78±12.73 % after 72 h (Fig. 2). Cells soaked in CAVICIDE™ (positive control) yielded no cell growth after both 48 and 72 h. After 48 h, the mean percent coverage of bacteria electroporated at 12.5, 15, and 17.5 kV/cm was 1.833±0.803 %, 2.248±1.503 %, and 0.223 ±0.387 %, respectively. After 72 h, the mean percent coverage of bacteria electroporated at 12.5, 15, and 17.5 kV/cm was 20.04±5.124 %, 8.122±3.400 %, and 0.650±0.545 %, respectively.

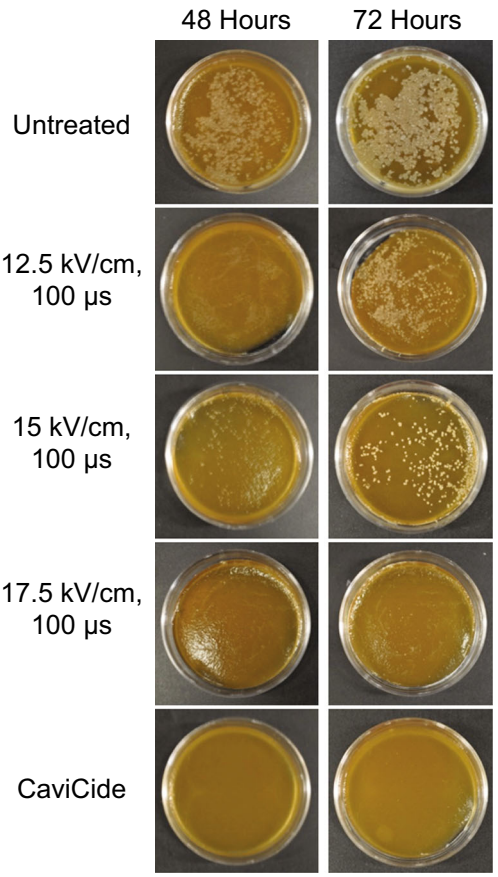

Fig. 1 Macroscopic images of bacteria seeded on agar plates taken after 48 and 72 h from initial seeding. Untreated bacteria (negative control), treated with CAVICIDE™ (positive control), and samples corresponding to treatments with an applied electric field of 12.5, 15, and 17.5 kV/cm are shown. There is an inverse relationship between percent coverage of agar and electric field magnitude used for IRE

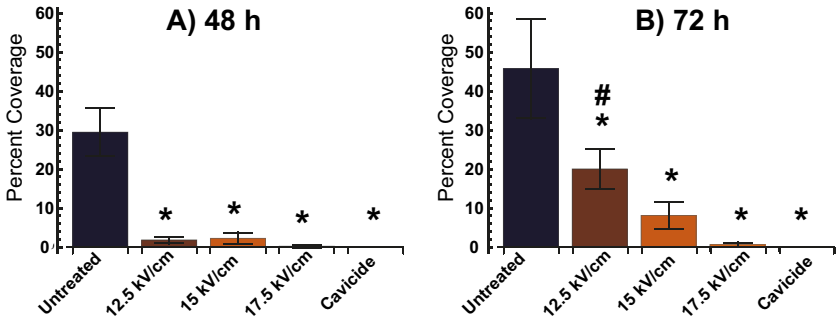

Fig. 2 Percent coverage of bacteria samples treated with IRE and seeded on agar plates (n=3) analyzed at **a** 48 h and **b** 72 h. *$p<0.05$ indicates statistical difference from the untreated bacteria (negative control) and #$p<0.05$ denotes statistical difference from bacteria soaked in CAVICIDE™ (positive control)

All of the treatments, including the positive control, were statistically different from the untreated cells (negative control) after 48 h. However, there was no statistical difference between any of the treatments and the positive control. After 72 h, all of the treatments, including the positive control, were again statistically different from the negative control. Cells electroporated at 12.5 kV/cm were also statistically different from cells electroporated at 17.5 kV/cm and cells soaked in CAVICIDE™ (positive control) after 72 h. However, there was no significant statistical difference for bacteria electroporated at 15 and 17.5 kV/cm and cells soaked in CAVICIDE™ (positive control) after 72 h.

Analytical solution and numerical model of lesion area

The analytical solution (Eq. 4) and the numerical solution of the local electric field distribution *E(x,y)* experienced by the pellicle were compared (Fig. 3). Solutions were given for the local electric field distribution experienced by the pellicle along the *y*-axis (*x*=0) for the applied electric field 10 kV/cm and 1 mm electrode spacing. The numerical solution and analytical solution are in good agreement (Fig. 3). A FEA model shows the mapping of the numerical solution of *E(x,y)* on the pellicle for an applied electric field of 10 and 12.5 kV/cm for 1 mm electrode spacing configuration (Fig. 4). The field contour lines represent the electric field threshold needed to create a 2–3 mm lesion area for an applied electric field of 10 and 12.5 kV/cm.

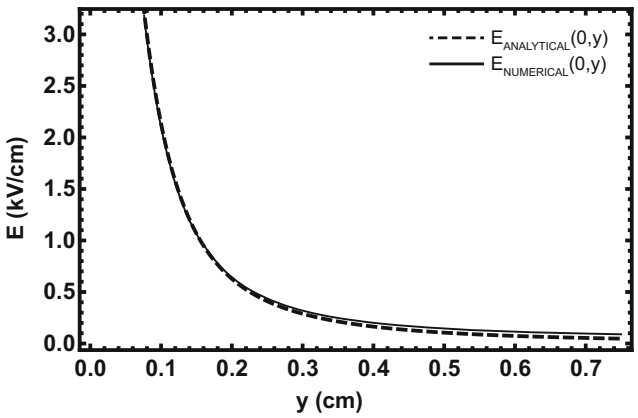

Fig. 3 FEA model of IRE can accurately predict the electric field distribution on cellulose samples. Comparison of analytical and numerical solutions of the electric field distribution along *y*-axis (*x*=0) for an E_field of 10 kV/cm shows a discrepancy of <10 % for *y*<3 mm, which is the region of interest

Creation of pores in BC scaffold

Macroscopic images (Figs. 5 and 6) and FESEM images (Figs. 7 and 8) were taken of treated pellicles. Table 1 below shows the different treatments applied to each group, appropriate lesion size, and approximate threshold. The mean±SD was determined for each treatment group where *n*=3.

Discussion

To determine cell death threshold, suspended bacteria were electroporated in cuvettes at electric field ratios ranging from 12.5 to 17.5 kV/cm and then seeded on agar plates. Looking at the theory of bacterial growth, a bacterium experiences a lag phase, an exponential growth phase, and eventually a stationary phase. For the exponential phase where most of the growth occurs, the growth rate equation for a specific species of bacteria can be described by the following equation:

$$N = N_0 e^{\mu t} \tag{7}$$

where N is the number of cells, N_0 is the initial seeding cell number, μ is the growth rate of a species of bacteria, and t is the elapsed time (Widdel 2007). Because the growth rate is specific to a species of bacteria, μ is defined by the following equation:

$$\mu = \frac{\ln 2}{t_d} \tag{8}$$

where t_d is the doubling time of the bacteria species (Widdel 2007). *G. xylinus* has a doubling time of 8–10 h in static

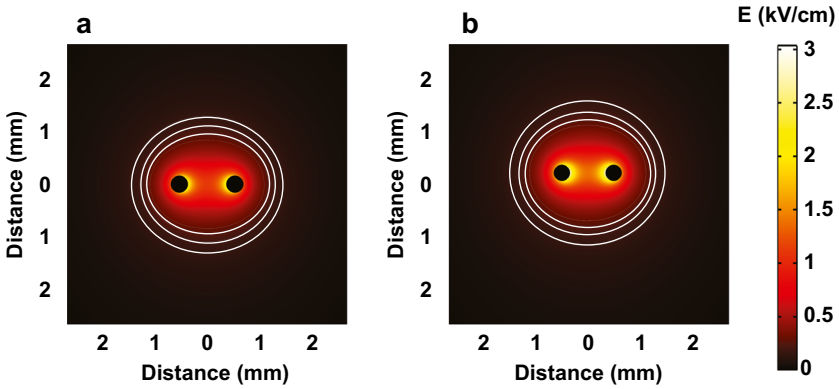

Fig. 4 FEA model describing the electric field distribution experienced on the bacterial cellulose at **a** 1000 V and **b** 1250 V delivered across a pair of needle electrodes spaced 1 mm apart. *Contour lines* represent the electric field at 2.5, 2, and 1.5 kV/cm, respectively, starting from the contour field closest to the pair of electrodes and moving outward

culture (Chawla et al. 2009). Specifically for *G. xylinus*, the calculated growth rate is approximately 8.66×10^{-2} h^{-1}. We assume that a viable bacterium cell can divide and produce colonies and possibly extracellular material on the agar plate and that a non-viable or dead cell will produce nothing after initial seeding. We also assume that 0 % coverage represents completely non-viable cells that did not produce any colonies or any extracellular material on the agar plate and therefore exhibit 0 % coverage of the agar plate. The untreated bacteria (negative control) exhibited approximately 30 % coverage after 48 h and 46 % coverage after 72 h. As the applied electric field increased, there was a noticeable decline in the percent coverage of bacteria. After 48 h, all electroporation treatments and the bacteria soaked in CAVICIDE™ (positive control) were statistically different from the untreated bacteria (negative control). The lack of statistical significance between electroporation treatments and bacteria soaked in CAVICIDE™ may be due to the short incubation period of 48 h, where no significant differences between treatments and the positive control were observed. However, there are statistical differences between treatments and the positive control after the 72 h time point, with the 12.5 kV/cm treatment showing statistical difference from the 17.5 kV/cm treatment and cells soaked in CAVICIDE™. Even though the 15 kV/cm treatment, 17.5 kV/cm treatment, and the cells soaked in CAVI CIDE™ were not statistically different, bacteria treated at 17.5 kV/cm exhibited the closest lack of coverage, with <0.5 % coverage after 48 h and <1 % coverage after 72 h.

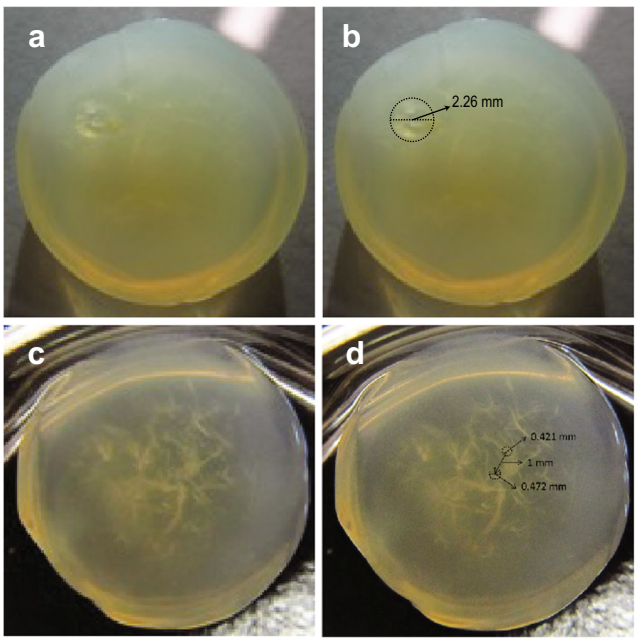

Fig. 5 A pore of ≈ 2.26 mm in diameter was successfully created on cellulose sample after IRE treatment with 90, 10-μs-long pulses delivered every second at **a** 800 V every hour for 24 h, and at 1000 V every hour for 48 h. **b** Measurement of lesion shown in **a**. No damage is observed on the untreated control sample as shown in **c** and **d** with electrode measurement

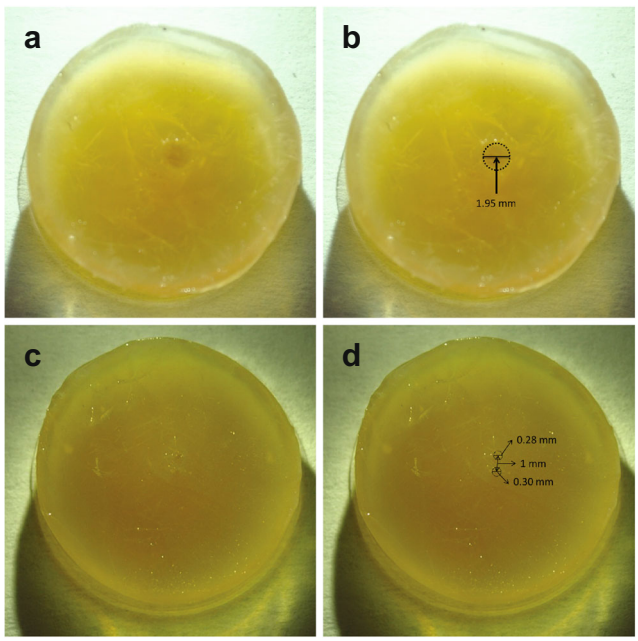

Fig. 6 A pore of ≈ 1.95 mm in diameter was successfully created on cellulose sample after IRE treatment with 90, 10-μs-long pulses delivered every second at **a** 1000 V every hour for 20 h, and at 800 V every hour for 52 h. **b** Measurement of lesion shown in **a**. No damage is observed on the untreated control sample as shown in **c** and **d** with electrode measurement

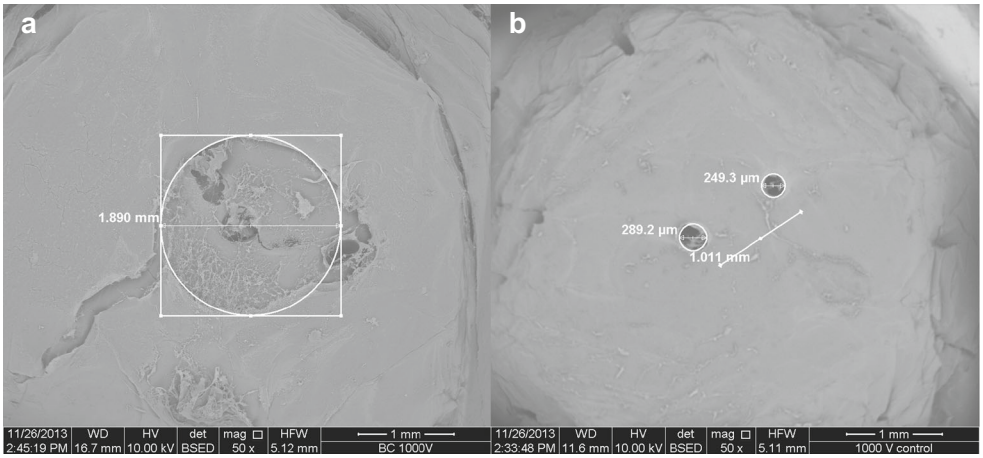

Fig. 7 An applied electric field of 10 kV/cm causes a lesion of ≈ 2 mm in the cellulose sample. **a** SEM image of cellulose sample treated with 90, 10-µs-long pulses of 1000 V, delivered with 1 s interval, every 15 min for 72 h using a pair of needle electrodes spaced 1 mm apart. **b** No damage is observed on the untreated cellulose sample (control) except for the area where the electrodes are placed

These results are comparable to cells soaked in CAVICIDE™ (positive control) and show that, with the correct set of parameters, IRE is a viable technique to kill *G. xylinus*. Knowing the IRE parameters required to kill *G. xylinus* can be very useful when trying to determine the IRE parameters needed to kill other species of bacteria. If another strain of bacteria has a similar shape, size, and membrane thickness as *G. xylinus*, one could use these parameters as a starting point to determine the parameters needed for a successful IRE treatment of the new strain.

The FEA model developed to determine the electric field threshold necessary to create conduits of particular sizes for treatments using a 1 mm electrode-spacing configuration showed the discrepancy between numerical and analytical solutions increases outside the electrodes ($y>$ 3 mm). The numerical solution is a slight overestimation of the analytical solution. However, for $y<3$ mm, which contains the region of interest for the lesions created, the discrepancy between the numerical and analytical solutions is <10 %. This proves that the numerical model accurately depicts the electric field distribution experienced on the pellicle for the region of interest.

The field contour maps (Fig. 4) represent the plotted numerical solution of the electric field distribution and predict the lesion area created on the surface of the pellicle, which can be compared to the macroscopic and FESEM images of the BC. Results show that samples in group 2 and group 3 experienced a lesion size of ≈ 2 mm. Comparing the images to the FEA model for the applied electric field 10 kV/cm (Fig. 4a), a lesion size of approximately 2 mm correlates to a threshold of 2.2 kV/cm. This shows that any bacteria that experienced a constant exposure of a local electric field of 2.2 kV/cm or higher every hour for 72 h were lysed, allowing the formation of a 2 mm pore. Samples in group 4 caused a lesion size of ≈ 2.5 mm. Thus, an applied electric field of 12.5 kV/cm causes a lesion of ≈ 2.5 mm as compared to the control where there is no damage in the absence of electric field. Similarly, comparing the images to the FEA model for the applied electric field of 12.5 kV/cm (Fig. 4b), a lesion size of approximately 2.5 mm corresponds to a threshold of 1.7 kV/cm. Thus, any bacteria that experienced a constant exposure of 1.7 kV/cm or higher every 30 min for 12 h were lysed, allowing the formation of the 2.5 mm pore. Bacteria outside the threshold field were not affected, allowing cellulose production to continue

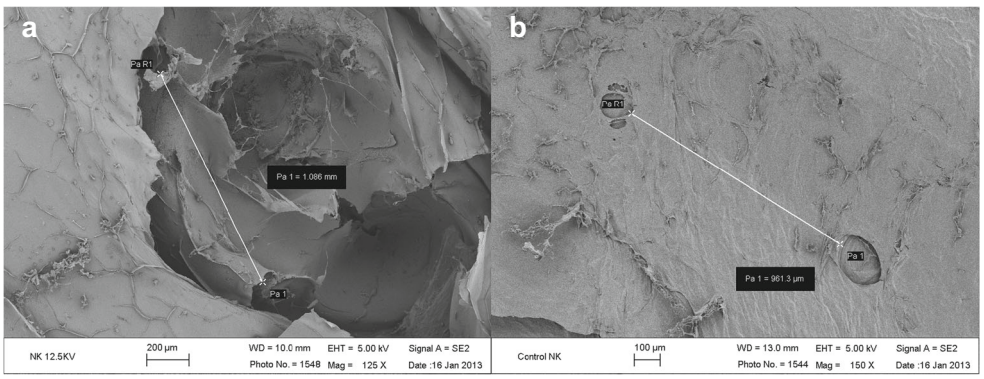

Fig. 8 An applied electric field of 12.5 kV/cm causes a lesion of ≈ 2.5 mm in cellulose sample as can be observed in **a** SEM image of cellulose sample treated with 90 pulses of 1250 V, each lasting 10 µs, with 1 s interval, delivered every 30 min for 12 h using a pair of needle electrodes spaced 1 mm apart. **b** No damage is observed on the control sample (cultured with uncharged electrodes during the 12-h period)

Table 1 Different treatment groups for creation of pores through IRE on BC scaffolds. The number of pulses (90), interval between pulses (1 s), and duration of pulse (10 μs) were kept constant. Lesion size means and standard deviations are reported and correlated to a particular electric field threshold value (n = 3). Example lesions from each group are shown in Figs. 5, 6, 7, and 8

Group	First pulse period		Second pulse period		Lesion size (mean±SD, mm)	Threshold (kV/cm)	Fig. #
1	800 V	Every hour for 24 h	1000 V	Every hour for 48 h	2.26±0.13	1.8	Fig. 5
2	1000 V	Every hour for 20 h	800 V	Every hour for 52 h	1.96±0.12	2.2	Fig. 6
3	1000 V	Every 15 min for 72 h	N/A	N/A	1.83±0.07	2.5	Fig. 7
4	1250 V	Every 30 min for 12 h	N/A	N/A	2.59±0.08	1.7	Fig. 8

around this area. All of the treatment groups also exhibit very low standard deviations, which shows that the set of parameters used in each group created a very similar sized lesion. These results validate the reproducibility of the IRE technique for creating conduits of a particular size.

Pulse parameters and experimental conditions greatly affect cell death; this is seen by the different cell death thresholds obtained from the in vitro experiments of bacteria treated in suspension (without cellulose present) and from the samples of bacteria treated during cellulose production. Because this is a proof-of-concept study, pulse parameters for the samples treated during cellulose production were varied to determine the possibility of a pore being formed. Based on the information provided by the FEA model, the electric field threshold needed to create a pore was established using multiple treatments. Bacteria cells are in suspension of growth media when pellicles are forming, making them active cultures. The in vitro studies were performed to determine the absolute threshold needed to kill bacteria based on a single treatment. However, applying these higher electric fields to the pellicle treatments produced too high of a current which resulted in sparking. This led us to determine equivalent pulse parameters needed to kill bacteria in a particular area to induce a pore. A study conducted by Pucihar et al. proved that with longer pulses or higher number of pulses, lower amplitudes are needed to cause cell death in the same fraction of electroporated cells (Pucihar et al. 2011). This is also the case for this set of experiments. Bacteria cells in suspension were treated with one continuous set of 1000 pulses, whereas the pellicles experienced 90 pulses every 15, 30, or 60 min over a period of 12 to 72 h. The larger amount of pulses experienced by the growing pellicle caused a lower threshold needed to kill bacteria, allowing for conduit formation. If one wanted to kill the bacteria by administering only one treatment, a much higher electric field would need to be applied, which is evident by the in vitro results of cells treated in suspension and plated on agar plates.

In this proof of concept study, we successfully showed that controlled IRE prevented cellulose deposition in a particular area, thus creating a local conduit in the scaffold by lysing bacteria. An applied electric field of 8–10 kV/cm causes a lesion of ≈ 2 mm in the cellulose sample, whereas an applied electric field of 12.5 kV/cm causes a lesion of ≈ 2.5 mm. By varying certain parameters such as the voltage applied, number of pulses, frequency, and duration between treatments, we show the creation of a localized pore in the scaffold, which can then lead to the creation of interconnecting conduits. Future work would be to automate and refine this fabrication process in order to develop custom-made scaffolds with various porosity densities to satisfy the requirements for orthopedic implants and other applications. We propose an automated approach to creating the conduits in a 3D microarchitecture, much like how 3D stereolithographic printing works. Cellulose is produced at the liquid/air interface, as such the BC pellicle grows from the bottom up in a controlled predictable manner that allows for a layer-by-layer fabrication process in which the electric pulses are delivered to the growing surface of the cellulose pellicle produced by bacteria. As each layer of BC is developed, a multi-head composed of an array of micro-electrodes will deliver the desired IRE treatment. These directed pulses would create a negative print or void in these locations; the pulse defines the area for bacteria lysing where no cellulose will be produced. This would allow for controllable pore distribution in the pellicle or XY-surface. Pore size is controlled via the voltage delivered and time duration for each pulse. As each layer or slice develops, the print head would ascend in the Z direction via an accurately coordinated servomotor, alternating pulse location, and void formations. The array of micro-electrodes would rotate via step motors to vary the location of pores within the scaffold. This would allow for controlled porosity and a gradient scaffold to be created. Furthermore, this automated approach could be implemented with magnetoporation and photoporation. These are relatively new techniques that could provide the means to lyse bacteria and create pores without requiring direct contact of the cellulose pellicle with electrodes. Magnetoporation employs a contactless treatment to kill cells by using pulsed magnetic fields (Novickij et al. 2014), and photoporation uses a short pulsed laser beam to induce cell damage (Xiong et al. 2014).

There are other techniques that could be used to create pores in a BC scaffold. One possible mechanism is the generation of pH fronts emerging from electrodes that cause bacteria to migrate to areas more similar to their natural

environment (Maglietti et al. 2013; Turjanski et al. 2011). Unlike IRE, this technique would not kill bacteria but would most likely cause bacteria to migrate and produce cellulose in areas not affected by the pH front. Another mechanism for creating pores could be through the use of dielectrophoresis (DEP), which uses a non-uniform electric field to induce polarization and move particles. Using interdigitated electrodes, one could employ a lower level AC field to repel bacteria from high field gradients using negative DEP. By strategically charging certain electrodes, an interconnected tube formation from the bottom to the top of the BC scaffold could be created. A study conducted by Zaborowska et al. showed the incorporation of wax paraffin microspheres into the fermentation process of *G. xylinus* to create pores in bacterial cellulose scaffolds (Zaborowska et al. 2010). The advantages of using wax paraffin microspheres to create pores in a BC scaffold are the ease of fabrication of wax microspheres, the ease of the removal of wax microspheres from the BC scaffold, and the control of the size distribution of the microspheres synthesized. This allows the researcher to create a range of sizes of microspheres to create a variable microporous scaffold. However, this technique does not provide a way to create interconnecting pores, which are essential for proper cell signaling, migration, and differentiation, as well as to provide a continuous pathway for a micro vessel to form. IRE potentially provides a solution to creating interconnecting pores. Ideally, as the cellulose grows, pulse parameters can be varied to produce a variable size conduit. A study conducted by Sano et al. used electrokinetic forces to stimulate and control bacterial motion of *G. xylinus* to fabricate customizable networks of cellulose nanofibrils (Sano et al. 2010). Although this work shows how to create a BC scaffold with tunable mechanical properties by controlling the alignment of the cellulose nanofibrils, it does not include an approach to incorporate porosity in this network. This study by Sano et al. can complement our study by using it to tailor the mechanical properties of the BC scaffold and using IRE to create interconnecting pores that can give way to microvasculature formation.

Tissue engineering, through the use of scaffolds, holds great promise for treating some of the most devastating diseases of our time. The major challenge thus far is attributed to the manufacturing of stable and functional 3D tissue structures, with appropriate porosity and microvasculature, to allow long-term viability of complex organs such as bone. In this study, we presented the feasibility of an approach to incorporate conduits into the cellulose scaffold through the use of IRE. The results suggest that IRE coupled with BC biofabrication could be an innovative technique to create scaffolds with pores and potentially conduits for tissue engineering applications. Our approach could allow for high degree of control over the bulk lattice structure which can result in better constructs with native tissue architecture.

Acknowledgments The authors acknowledge NIH R43 AG044153-01A1, NSF 1026421, and the NSF IGERT DGE-0966125, MultiSTEPS for support of this research. We also would like to thank Dr. Christopher Arena for compiling the computer program that controlled the delivery of the electrical pulses and Lisa Anders for helping assemble the MATLAB script for image analysis.

References

Azuma C, Yasuda K, Tanabe Y, Taniguro H, Kanaya F, Nakayama A, Chen YM, Gong JP, Osada Y (2007) Biodegradation of high-toughness double network hydrogels as potential materials for artificial cartilage. J Biomed Mater Res A 81:373–380. doi:10.1002/jbm.a.31043

Bodin A, Backdahl H, Fink H, Gustafsson L, Risberg B, Gatenholm P (2007) Influence of cultivation conditions on mechanical and morphological properties of bacterial cellulose tubes. Biotechnol Bioeng 97:425–434. doi:10.1002/bit.21314

Chawla PR, Bajaj IB, Survase SA, Singhal RS (2009) Microbial cellulose: Fermentative production and applications. Food Technol Biotechnol 47:107–124

Corovic S, Pavlin M, Miklavcic D (2007) Analytical and numerical quantification and comparison of the local electric field in the tissue for different electrode configurations. Biomed Eng Online 6:37. doi:10.1186/1475-925x-6-37

Czaja WK, Young DJ, Kawecki M, Brown RM Jr (2007) The future prospects of microbial cellulose in biomedical applications. Biomacromolecules 8:1–12. doi:10.1021/bm060620d

Davalos RV, Mir LM, Rubinsky B (2005) Tissue ablation with irreversible electroporation. Ann Biomed Eng 33:223–231

Ellis DL, Yannas IV (1996) Recent advances in tissue synthesis in vivo by use of collagen-glycosaminoglycan copolymers. Biomaterials 17:291–299

Garcia PA, Pancotto T, Rossmeisl JH Jr, Henao-Guerrero N, Gustafson NR, Daniel GB, Robertson JL, Ellis TL, Davalos RV (2011) Non-thermal irreversible electroporation (N-TIRE) and adjuvant fractionated radiotherapeutic multimodal therapy for intracranial malignant glioma in a canine patient. Technol Cancer Res Treat 10:73–83

Gauvin R, Chen YC, Lee JW, Soman P, Zorlutuna P, Nichol JW, Bae H, Chen S, Khademhosseini A (2012) Microfabrication of complex porous tissue engineering scaffolds using 3D projection stereolithography. Biomaterials 33:3824–3834. doi:10.1016/j.biomaterials.2012.01.048

Gimsa J, Wachner D (2001) Analytical description of the transmembrane voltage induced on arbitrarily oriented ellipsoidal and cylindrical cells. Biophys J 81:1888–1896

Gusbeth C, Frey W, Volkmann H, Schwartz T, Bluhm H (2009) Pulsed electric field treatment for bacteria reduction and its impact on hospital wastewater. Chemosphere 75:228–233. doi:10.1016/j.chemosphere.2008.11.066

Harris LD, Kim BS, Mooney DJ (1998) Open pore biodegradable matrices formed with gas foaming. J Biomed Mater Res 42:396–402

Helenius G, Bäckdahl H, Bodin A, Nannmark U, Gatenholm P, Risberg B (2006) In vivo biocompatibility of bacterial cellulose. J Biomed Mater Res Part A 76A:431–438. doi:10.1002/jbm.a.30570

Karageorgiou V, Kaplan D (2005) Porosity of 3D biomaterial scaffolds and osteogenesis. Biomaterials 26:5474–5491. doi:10.1016/j.biomaterials.2005.02.002

Katz JN, Losina E (2013) Surgery versus physical therapy for meniscal tear and osteoarthritis. N Engl J Med 369:677–678. doi:10.1056/NEJMc1307177

Kotnik T, Miklavcic D (2000) Analytical description of transmembrane voltage induced by electric fields on spheroidal cells. Biophys J 79: 670–679. doi:10.1016/S0006-3495(00)76325-9

Maglietti F, Michinski S, Olaiz N, Castro M, Suarez C, Marshall G (2013) The role of ph fronts in tissue electroporation based treatments. PLoS ONE 8:e80167. doi:10.1371/journal.pone.0080167

Matthews JA, Wnek GE, Simpson DG, Bowlin GL (2002) Electrospinning of collagen nanofibers. Biomacromolecules 3: 232–238

Mello LR, Feltrin LT, Neto PTF, Ferraz FAP (1997) Duraplasty with biosynthetic cellulose: an experimental study. J Neurosurg 86:143–150. doi:10.3171/Jns.1997.86.1.0143

Mooney DJ, Mikos AG (1999) Growing new organs. Sci Am 280:60–65

Murphy CM, Haugh MG, O'Brien FJ (2010) The effect of mean pore size on cell attachment, proliferation and migration in collagen-glycosaminoglycan scaffolds for bone tissue engineering. Biomaterials 31:461–466. doi:10.1016/j.biomaterials.2009.09.063

Neal RE 2nd, Singh R, Hatcher HC, Kock ND, Torti SV, Davalos RV (2010) Treatment of breast cancer through the application of irreversible electroporation using a novel minimally invasive single needle electrode. Breast Cancer Res Treat 123:295–301. doi:10.1007/s10549-010-0803-5

Novickij V, Grainys A, Novickij J, Markovskaja S (2014) Irreversible magnetoporation of micro-organisms in high pulsed magnetic fields. IET Nanobiotechnol 8:157–162. doi:10.1049/iet-nbt.2013.0005

Petersen N, Gatenholm P (2011) Bacterial cellulose-based materials and medical devices: current state and perspectives. Appl Microbiol Biotechnol 91:1277–1286. doi:10.1007/s00253-011-3432-y

Place ES, George JH, Williams CK, Stevens MM (2009) Synthetic polymer scaffolds for tissue engineering. Chem Soc Rev 38:1139–1151. doi:10.1039/b811392k

Pucihar G, Krmelj J, Rebersek M, Napotnik TB, Miklavcic D (2011) Equivalent pulse parameters for electroporation. IEEE Trans Biomed Eng 58:3279–3288. doi:10.1109/Tbme.2011.2167232

Sano MB, Rojas AD, Gatenholm P, Davalos RV (2010) Electromagnetically controlled biological assembly of aligned bacterial cellulose nanofibers. Ann Biomed Eng 38:2475–2484. doi:10.1007/s10439-010-9999-0

Schumann D, Wippermann J, Klemm D, Kramer F, Koth D, Kosmehl H, Wahlers T, Salehi-Gelani S (2009) Artificial vascular implants from bacterial cellulose: Preliminary results of small arterial substitutes. Cellulose 16:877–885. doi:10.1007/s10570-008-9264-y

Sobrino-Lopez A, Martin-Belloso O (2006) Enhancing inactivation of *Staphylococcus aureus* in skim milk by combining high-intensity pulsed electric fields and nisin. J Food Prot 69:345–353

Toepfl S, Mathy A, Heinz V, Knorrr D (2006) Review: Potential of high hydrostatic pressure and pulsed electric field for energy efficient and environmentally friendly food processing. Food Rev Int 22:405–423

Turjanski P, Olaiz N, Maglietti F, Michinski S, Suarez C, Molina FV, Marshall G (2011) The role of pH fronts in reversible electroporation. PLoS ONE 6:e17303. doi:10.1371/journal.pone.0017303

Widdel F (2007) Theory and measurement of bacterial growth. Di dalam Grundpraktikum Mikrobiologie 4:1-11

Xiong R, Raemdonck K, Peynshaert K, Lentacker I, De Cock I, Demeester J, De Smedt SC, Skirtach AG, Braeckmans K (2014) Comparison of gold nanoparticle mediated photoporation: Vapor nanobubbles outperform direct heating for delivering macromolecules in live cells. ACS Nano 8:6288–6296. doi:10.1021/nn5017742

Yamanaka S, Watanabe K, Kitamura N, Iguchi M, Mitsuhashi S, Nishi Y, Uryu M (1989) The structure and mechanical-properties of sheets prepared from bacterial cellulose. J Mater Sci 24:3141–3145. doi:10.1007/Bf01139032

Yang S, Leong KF, Du Z, Chua CK (2001) The design of scaffolds for use in tissue engineering. Part I. Traditional factors. Tissue Eng 7:679–689. doi:10.1089/107632701753337645

Yoon SH, Jin HJ, Kook MC, Pyun YR (2006) Electrically conductive bacterial cellulose by incorporation of carbon nanotubes. Biomacromolecules 7:1280–1284. doi:10.1021/bm050597g

Zaborowska M, Bodin A, Backdahl H, Popp J, Goldstein A, Gatenholm P (2010) Microporous bacterial cellulose as a potential scaffold for bone regeneration. Acta Biomater 6:2540–2547. doi:10.1016/J.Actbio.2010.01.004